Acta Pharmaceutica Sinica B 2020;10(2):344−357

Chinese Pharmaceutical Association
Institute of Materia Medica, Chinese Academy of Medical Sciences

Acta Pharmaceutica Sinica B

www.elsevier.com/locate/apsb
www.sciencedirect.com

ORIGINAL ARTICLE

# Improving the positional adaptability: structure-based design of biphenyl-substituted diaryltriazines as novel non-nucleoside HIV-1 reverse transcriptase inhibitors

**Kaijun Jin[a,b,†], Minjie Liu[a,b,†], Chunlin Zhuang[a,b], Erik De Clercq[c], Christophe Pannecouque[c], Ge Meng[a,b,*], Fener Chen[a,b,*]**

[a]*Engineering Center of Catalysis and Synthesis for Chiral Molecules, Department of Chemistry, Fudan University, Shanghai 200433, China*
[b]*Shanghai Engineering Center of Industrial Asymmetric Catalysis for Chiral Drugs, Shanghai 200433, China*
[c]*Rega Institute for Medical Research, KU Leuven, Leuven B-3000, Belgium*

Received 8 February 2019; received in revised form 8 July 2019; accepted 20 September 2019

**KEY WORDS**

HIV-1;
NNRTIs;
NP-DATAs;
BP-DATAs;
Positional adaptability;
Molecular modeling

**Abstract** In order to improve the positional adaptability of our previously reported naphthyl diaryltriazines (NP-DATAs), synthesis of a series of novel biphenyl-substituted diaryltriazines (BP-DATAs) with a flexible side chain attached at the C-6 position is presented. These compounds exhibited excellent potency against wild-type (WT) HIV-1 with $EC_{50}$ values ranging from 2.6 to 39 nmol/L and most of them showed low nanomolar anti-viral potency against a panel of HIV-1 mutant strains. Compounds **5j** and **6k** had the best activity against WT, single and double HIV-1 mutants and reverse transcriptase (RT) enzyme comparable to two reference drugs (EFV and ETR) and our lead compound NP-DATA (**1**). Molecular

*Abbreviations:* AIDS, acquired immunodeficiency syndrome; BP-DATA, biphenyl-substituted diaryltriazine; $CC_{50}$, 50% cytotoxicity concentration; DAPY, diarylpyrimidine; DATA, diaryltriazine; EFV, efavirenz; ETR, etravirine; $EC_{50}$, the concentration causing 50% inhibition of antiviral activity; HEPT, 1-[(2-hydroxyethoxy)methyl]-6-(phenylthio)thymine; HIV, human immunodeficiency virus; MD, molecular dynamic; NNRTI, non-nucleoside reverse transcriptase inhibitor; NNIBP, non-nucleoside inhibitor binding pocket; NP-DATA, naphthyl diaryltriazine; NVP, nevirapine; PK, pharmacokinetics; RPV, rilpivirine; RMSD, root-mean square deviation; RT, reverse transcriptase; SAR, structure−activity relationship; SI, selectivity index; TSAO, *tert*-butyldimethylsilyl-spiroaminooxathioledioxide; WT, wild-type.

*Corresponding authors. Tel./fax: +86 21 65643811.
E-mail addresses: mgfudan@fudan.edu.cn (Ge Meng), rfchen@fudan.edu.cn (Fener Chen).

†These authors made equal contributions to this work.

Peer review under responsibility of Institute of Materia Medica, Chinese Academy of Medical Sciences and Chinese Pharmaceutical Association.

https://doi.org/10.1016/j.apsb.2019.09.007

modeling disclosed that the side chain at the C-6 position of DATAs occupied the entrance channel of the HIV-1 reverse transcriptase non-nucleoside binding pocket (NNIBP) attributing to the improved activity. The preliminary structure−activity relationship and PK profiles were also discussed.



## 1. Introduction

Non-nucleoside reverse transcriptase inhibitors (NNRTIs) are the crucial components of the highly active antiretroviral therapy (HAART) to treat acquired immunodeficiency syndrome (AIDS) caused by human immune deficiency virus 1 (HIV-1)[1,2]. To date, more than 60 types of structure skeletons have been reported as NNRTIs[3−5], sharing the advantages of high potency, low toxicity and exquisite selectivity, and favorable pharmacokinetics for targeting at the allosteric non-nucleoside binding pocket (NNIBP) of the reverse transcriptase (RT)[6,7]. This site is located 10–15 Å away from the active catalytic site of DNA polymerase of HIV-1 RT[8], which is composed of three main portions including an entrance channel (Lys101, Lys 103, Glu138, Val179, etc.), a groove site (Val106, His235, Pro236, Pro226, Pro225, Phe227, etc.) and a tunnel site (Trp229, Tyr188, Tyr181, etc.)[9−11]. The binding conformations of these various NNRTIs within NNIBP are different, *e.g.*, "butterfly" for 1-[(2-hydroxyethoxy)methyl]-6-(phenylthio)thymines (HEPTs) and nevirapine (NVP)[12], "seahorse" for diaryltriazines (DATAs)[13], "horseshoe" for diarylpyrimidines (DAPYs) and "dragon" for the *tert*-butyldimethylsilyl-spiroaminooxathioledioxide (TSAO)[14]. Thus, the variety and binding conformations could offer many opportunities for further structural optimizations[15,16]. As an important category of NNRTIs, DATAs share many similarities with DAPYs in their structural skeletons[17−19], biological activities and structure−activity relationships (SARs), especially in their flexible binding conformations to suit the allosteric NNIBP[20]. The adaptability could allow them, as well as two clinically used DAPYs (etravirine, ETR; rilpivirine, RPV)[19,21], to interact with the variable residues of NNIBP[19], making these compounds highly effective against wild-type (WT) and various mutant strains of HIV-1[13]. Nevertheless, the emerging drug resistance and the poor aqueous solubility of ETR (much lower than 1 μg/mL) and RPV (20 ng/mL at pH 7.0) inevitably limit the long-term clinical uses[22,23].

Based on a 3D-QSAR study of DATAs, our research group has conducted to attach a substituted ($\alpha$ or $\beta$)-naphthyl group to the 4-position of DATAs (NP-DATA, **1**)[19] and the $\pi-\pi$ stacking interactions with the aromatic residues in the tunnel site of NNIBP was increased[24−26]. In addition, introducing the biphenyl group to DAPYs have also been disclosed in our lab to increase the $\pi-\pi$ stacking interactions and antiviral activity[27−29]. Considering the structural similarity between DAPYs and DATAs, we hypothesized that introducing the biphenyl group at a similar position of DATAs might benefit their biological activity. On the other hand, the chemical space around the 6-position of DATAs, which is located at the entrance channel of HIV-1 RT, remains unexplored. Many kinds of modifications around the channel have been reported, making the target molecules improve antiviral activities as well as physicochemical properties[30]. The modifications commonly introduced some N-containing heterocycles, including both hydrogen-bond donors and acceptors, could increase the interactions with the possible mutants, such as K103N and E138K.

In this study, we designed a new series of DATAs with the purpose to improve the positional adaptability in the NNIBP (Fig. 1). Firstly, replacement of the naphthyl by biphenyl group at the 4-position through hybridization with biphenyl substituted-DAPY (**2**) could adapt the hydrophobic pocket of Trp229 and keep the $\pi-\pi$ stacking interactions with the aromatic residues in the tunnel site of NNIBP. Secondly, attaching the same 4-cyano phenyl amino group of ETR and RPV to the 2-position of DATAs maintains the binding with solvent-exposed area of NNIBP. In this study, the 4-cyano-biphenyl group and 4-cyanoaniline group, which have been determined to be favorable for the activity in our other studies[27−29] are constant in the final BP-DATA molecules. Thirdly and most importantly, introducing the different side chains at the 6-position of DATAs improves the ligand's adaptability with the entrance channel of NNIBP. Various flexible side chains are tried, such as rigid N-containing heterocycles and aliphatic esters, which could increase the number of rotatable bonds and enhance their adaptability and flexibility for binding to the various mutant types of HIV-1 RT.

## 2. Results and discussion

### 2.1. Synthesis of the target molecules

As depicted in Scheme 1, the target molecules were obtained. Briefly, the intermediates **3b** or **3b-1** and **3a** were synthesized following established procedures[27,29,31]. Nucleophilic substitution of **3a** with the intermediates **10** or **11** provided the key intermediates **4a** or **4b**, which were followed by nucleophilic substitution with various substituted amines to give the target compounds **5** or **6**. All the new compounds were fully characterized by infrared spectra (IR), high resolution mass spectrum (HRMS), proton nuclear magnetic resonance ($^1$H NMR) spectroscopy and carbon nuclear magnetic resonance ($^{13}$C NMR) spectroscopy.

### 2.2. Biological assays

#### 2.2.1. Anti-HIV activities in cells and SAR analysis

The anti-viral activity of all the target molecules against WT HIV-1 and ROD, as well as their activities against the HIV-1 mutant

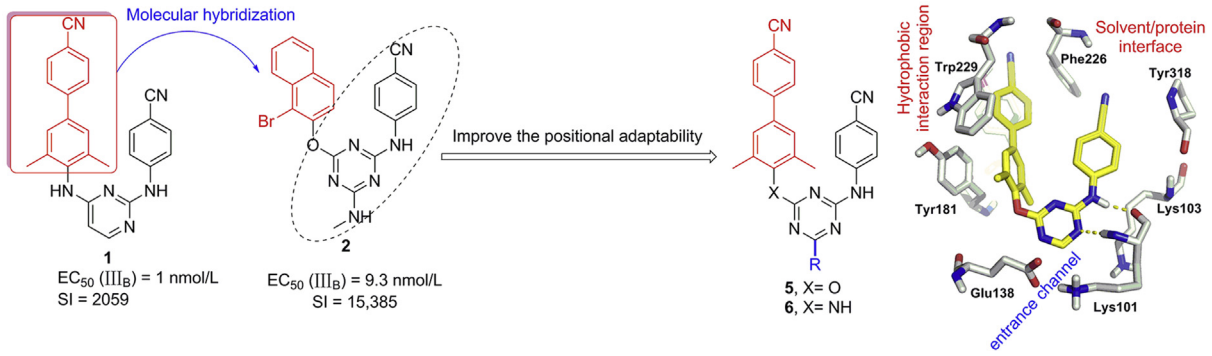


**Figure 1** The design of the BP-DATAs by molecular hybridization to improve the positional adaptability in the NNIBP.

strains, were evaluated to validate our hypothesis and investigate the preliminary SAR of these DATAs. The antiviral potency of all the target compounds was evaluated using HIV infected MT-4 cells. NVP, EFV and ETR were selected as the reference drugs. The values of $EC_{50}$ (anti-HIV potency), $CC_{50}$ (cytotoxicity) and SI (selectivity index, $CC_{50}/EC_{50}$ ratio) were summarized in Tables 1 and 2, respectively. The biological assay results indicated that all the new DATAs exhibited significant anti-viral potency against WT HIV-1 with low nanomolar $EC_{50}$ values of 2.6−39 nmol/L, which were more potent than NVP ($EC_{50}$ = 45 nmol/L) and lead DATA **1** ($EC_{50}$ = 9.3 nmol/L). Compound **6k** was the most potent with an $EC_{50}$ of 2.6 nmol/L, similar to ETR ($EC_{50}$ = 2.2 nmol/L) and EFV ($EC_{50}$ = 1 nmol/L). Furthermore, compound **6e** with a similar activity ($EC_{50}$ = 3.1 nmol/L) showed the lowest cytotoxicity ($CC_{50}$ > 125 μmol/L) and the highest selectivity index (SI > 40,000), which was superior to ETR ($CC_{50}$ > 2.0 μmol/L, SI > 909). Most of the target compounds showed excellent selectivity against the HIV-2 strain, except compound **5j** ($EC_{50}$ = 50 nmol/L).

SAR analysis indicated that: (1) as expected, the biphenyl and *p*-cyanoaniline groups were favorable to enhance the anti-viral activity. (2) The oxygen and nitrogen linker showed influence on the antiviral activity against HIV-1 and HIV-2 strains. The activity of the compounds with the nitrogen linker was better, for instance, **5b** with oxygen linker ($EC_{50}$ = 39 nmol/L) *vs.* **6c** with nitrogen linker ($EC_{50}$ = 11 nmol/L), **5k** *vs.* **6n**. The inhibitory activities ($EC_{50}$ values) against HIV-2 (ROD) of DATAs with the oxygen linker (−O− in **5a–5k**) seemed more potent than the compounds with the nitrogen linker (−NH− in **6a–6n**). (3) Compounds **5j** and **6m** with two more methylenes showed 10-fold and 2-fold higher activity than corresponding **5e** and **6g**. However, compounds with the methyl piperazine group (**5f** and **5k, 6h** and **6n**) exhibited a similar activity. Compounds **5h** and **6k** with the pyrrolidinol group had an anti-HIV-1 activity higher than those (**5g** and **6j**) with the pyrrolidinylmethanol group. (4) The properties of the substituents (R) at the C6-position of the triazine ring could also exert the dramatic effects on the pharmacological properties of the target compounds. Most compounds have the low cytotoxicity (**5a**, **5b**, **5c**, **6a**, **6b** and **6c**) and high SI (**6a** and **6e**), indicating that the substituents at the C6-position could increase their therapeutic safety.

Then, five compounds (**5h**, **5j**, **6e**, **6i** and **6k**) with $EC_{50}$ values lower than 3.5 nmol/L were selected to evaluate against the HIV-1 mutant strains (Table 2). They were more potent than NVP and comparable to EFV and ETR. Notably, **6k** was the most potent inhibitor with the antiviral efficacy against the single mutant equivalent to the potency of ETR. Compound **5j** exhibited great activity against the viral, especially the double mutant strains of HIV-1 K103N/Y181C and F227L/V106A with $EC_{50}$ values of 34 and 17 nmol/L, respectively.

### 2.2.2. *Anti-HIV RT and RT RNase H activities*

In order to validate the binding target of these newly synthesized compounds, the enzymatic assay was performed (Table 3). The results demonstrated that all the compounds displayed the good activity against WT HIV-1 RT with $IC_{50}$ values ranging from 0.033 to 0.368 μg/mL. Most compounds had better anti-RT activity ($IC_{50}$ < 0.1 μg/mL) than NVP and ETR. Compound **6b** showed excellent binding affinity with HIV-1 RT ($IC_{50}$ = 0.033 μg/mL). Then, the effect of the target compounds against HIV-1 RT RNase H was evaluated. Only three compounds (**5e**, **5i**, and **5h**) showed slight activity against RNase H sharing a similar structure feature of the oxygen linker. The above results indicated that the newly designed DATA compounds specifically targeted RT NNIBP but not RNase H binding site.

## 2.3. *Pharmacokinetics-associated studies*

### 2.3.1. *Solubility and lipophilic efficiency*

Next, the active compounds **5a**, **5j**, **6e**, **6i** and **6k** were chosen for further assessment of the certain physicochemical properties. The aqueous solubility, which is important for *in vivo* dosing formulation and bioavailability[32], was measured at three different pH values (7.4, 7.0 and 2.0) and fasted state simulated intestinal fluid (FaSSIF) (Table 4). The polar surface areas of the selected compounds are around 200 $Å^2$, which are similar to ETR (Table 5). All the tested compounds showed better solubility (S = 14.7–60.6 μg/mL) in FaSSIF than that of ETR (S = 13.2 μg/mL), suggesting the properties of good solubility in the intestinal environment.

### 2.3.2. *Cytochrome P450 enzymatic inhibitory activity*

It is reported that the NNRTIs mainly undergo metabolism *via* cytochrome P450 oxidative metabolism[33]. Therefore, the *in vitro* ability to inhibit CYP drug-metabolizing enzymes of the most active compound **5j** was evaluated (Table 5). It displayed no

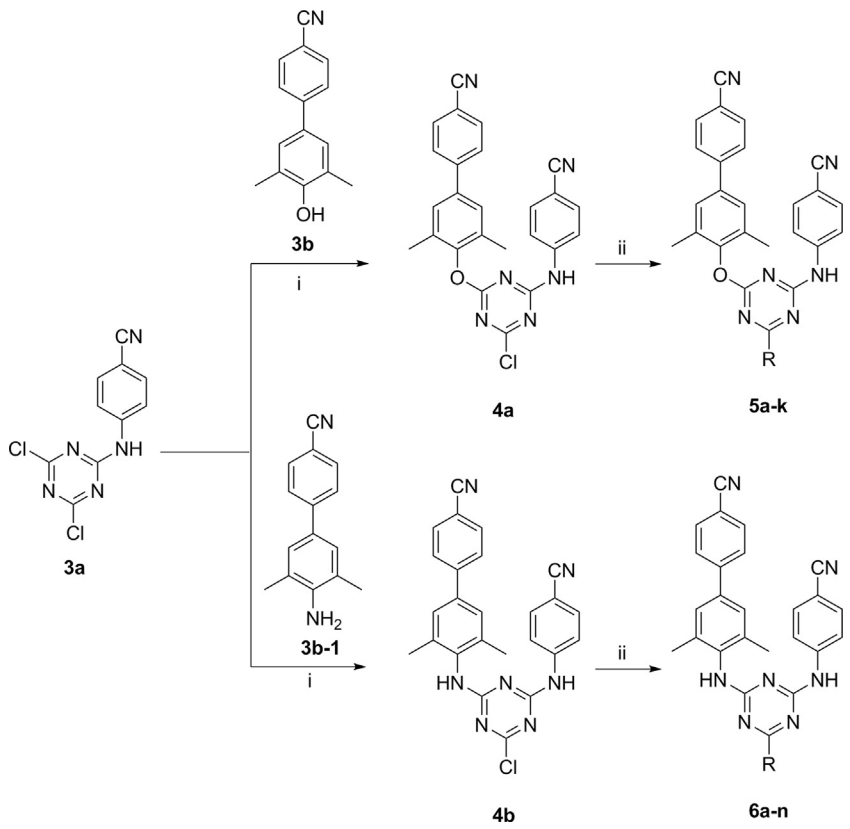


**Scheme 1** Reagents and conditions: (i) NaH, THF, 0 °C–r.t., or DIPEA, THF, reflux, 70%–80%; (ii) various substituted amines, $K_2CO_3$ or DIPEA, THF, r.t., 2–5 h, 60%–75%.

apparent inhibition of CYP1A2 ($IC_{50}$ > 50.0 μmol/L), CYP2C9 ($IC_{50}$ = 32.9 μmol/L), CYP2C19 ($IC_{50}$ > 50.0 μmol/L), CYP2D6 ($IC_{50}$ > 50.0 μmol/L), and CYP3A4M ($IC_{50}$ > 50.0 μmol/L), indicating its strength different from most NNRTIs.

### 2.3.3. *Determination of plasma protein binding rate*

Furthermore, **5j** was evaluated for its binding ability with human and rat plasma proteins with the dialysis equilibrium method. As shown in Table 6, the plasma protein binding rates of **5j** were higher than 99.9% in human and rat. The result demonstrated that the compound **5j** could bind strongly to plasma protein with a relatively low concentration of free drug, which needs for optimization in the future[34].

### 2.3.4. *In vivo pharmacokinetics study*

Considering its good potency against WT and mutant variants, pharmacokinetics (PK) properties of compound **5j** were evaluated in SD rats. After a single 2 mg/kg i.v. dose of **5j**, the mean clearance rate (CL) and half-time ($t_{1/2}$) were 5.06 mL/min·kg and 0.734 h, respectively (Table 7, Fig. 2 and Supporting Information Fig. S1). Absorption of **5j** was assessed after being orally dosed at 20 mg/kg; it reached maximum concentration ($T_{max}$) at 13.3 h with a maximum concentration ($C_{max}$) of 43.23 ng/mL. However, the oral bioavailability ($F$) was only 0.485%, which was very low requiring further modification. All methods and procedures of protocol were approved by the Animal Care and Use Committee of WuXi AppTec (Shanghai site).

## 2.4. *Molecular modelling*

To further understand the binding modes between these new DATAs and RT, we conducted molecular docking studies of the representative compounds **5j** and **6k** with Surflex Dock. The X-ray crystal structure of the WT HIV-1 RT (2ZD1) was used for the docking calculations. PyMOL software was used to analyze and visualize these docking results. Compounds **5j** and **6k** showed the similar binding conformations of horseshoe-shape as the traditional NNRTIs (Fig. 3). The biphenyl group fitted into the tunnel site of NNIBP, exhibiting the positive face-to-face $\pi-\pi$ stacking interactions, supporting its improved adaptability with the aromatic residues (*e.g.*, Tyr181, Tyr188 and Trp229). The nitrogen of the central ring and NH linker of these two compounds were involved in the crucial hydrogen-bonding interactions with the amide backbone of Lys101. The *p*-cyanoaniline extended to a solvent-exposed region of NNIBP surrounded by residues such as His235, Pro236 and Try318. The R substituents at the 6-position of DATA in compounds **5j** and **6k** occupied the entrance channel composed by Val106, Glu138 and Val179 residues. It is noteworthy that the 3-hydroxyl group attached to the pyrrole ring of the most active compound **6k** even extended outside of the entrance channel, which might be associated with its better biological activity (Fig. 3).

Although the most active inhibitors share similar binding conformations in the hydrogen-bonding and $\pi-\pi$ stacking interactions with RT (Fig. 3), the less active inhibitors showed different binding conformations with NNIBP (Fig. 4). The interaction between compound **5b** with NNIBP still involved two

**Table 1** Activity and cytotoxicity against HIV-1 ($III_B$) and HIV-2 (ROD) strains in MT-4 cells.

| Compd. | X | R | $EC_{50}$ (nmol/L)[a] | | $CC_{50}$ (μmol/L)[b] | SI (WT $III_B$)[c] |
|---|---|---|---|---|---|---|
| | | | HIV-1 WT IIIB | ROD | | |
| **5a** | O |  | 6.8 ± 2.1 | 560 ± 140 | >125.00 | >18,315 |
| **5b** | O |  | 39 ± 25 | 2030 ± 940 | >125.00 | >3213 |
| **5c** | O | 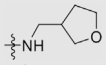 | 14 ± 4 | 1010 ± 210 | >125.00 | >9080 |
| **5d** | O | 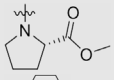 | 19 ± 6 | >2230 | 2.23 ± 1.09 | 119 |
| **5e** | O |  | 32 ± 3 | 3610 ± 550 | >125.00 | >3870 |
| **5f** | O |  | 21 ± 2 | >9800 | 9.80 ± 7.31 | 470 |
| **5g** | O | 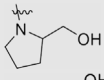 | 25 ± 14 | 1560 ± 490 | >125.00 | >4900 |
| **5h** | O | 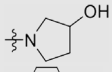 | 3.5 ± 0.6 | 2910 ± 980 | 5.72 ± 0.08 | 1635 |
| **5i** | O | 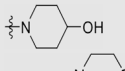 | 11 ± 5 | 1510 ± 260 | 14.86 ± 7.89 | 1402 |
| **5j** | O | 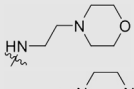 | 3.4 ± 0.9 | 50 ± 1 | 1.08 ± 0.09 | 318 |
| **5k** | O | 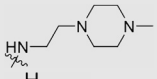 | 30 ± 7 | >14,090 | 14.09 ± 3.47 | 476 |
| **6a** | NH |  | 6.1 ± 2.3 | 26,460 ± 20,500 | >125.00 | >20,604 |
| **6b** | NH | 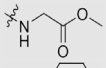 | 5.5 ± 2.7 | 21,460 ± 11,910 | >125.00 | >22,727 |
| **6c** | NH | 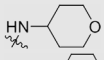 | 11 ± 5 | 40,010 ± 21,080 | >125.00 | >11,390 |
| **6d** | NH | 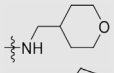 | 6.9 ± 1.9 | 13,780 ± 9070 | >125.00 | >18,029 |
| **6e** | NH | 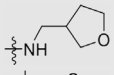 | 3.1 ± 0.9 | 7910 ± 5700 | >125.00 | >40,000 |
| **6f** | NH | 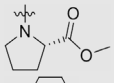 | 21 ± 4 | >125,000 | >125.00 | >5903 |
| **6g** | NH |  | 6.2 ± 0.8 | 39,940 ± 19,250 | >125.00 | >20,107 |
| **6h** | NH | 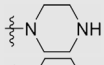 | 11 ± 5 | >9240 | 9.24 ± 5.50 | 814 |
| **6i** | NH | 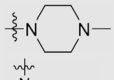 | 3.3 ± 0.6 | >3690 | 3.69 ± 2.98 | 1110 |
| **6j** | NH | 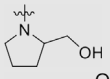 | 4.8 ± 0.9 | 15,700 ± 1230 | 62.86 ± 7.99 | 13,096 |
| **6k** | NH | 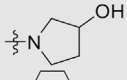 | 2.6 ± 0.4 | >4540 | 4.54 ± 2.56 | 1769 |
| **6l** | NH | 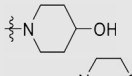 | 4.7 ± 1.7 | >5710 | 5.71 ± 3.93 | 1223 |
| **6m** | NH | 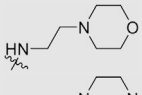 | 3.7 ± 0.6 | >13,870 | 13.87 ± 10.68 | 3801 |
| **6n** | NH | 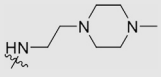 | 5 ± 1 | >2340 | 2.34 ± 0.64 | 469 |
| NVP | – | – | 45 ± 2 | >4000 | >4.0 | >90 |
| EFV | – | – | 1 ± 0.3 | – | >2.0 | >2000 |

**Table 1** (*continued*)

| Compd. | X | R | $EC_{50}$ (nmol/L)[a] | | $CC_{50}$ (μmol/L)[b] | SI (WT $III_B$)[c] |
|---|---|---|---|---|---|---|
| | | | HIV-1 WT IIIB | ROD | | |
| ETR[d] | – | – | 2.2 ± 0.3 | – | >2.0 | >909 |
| ETV | – | – | 2.2 ± 0.3 | – | >2.0 | >909 |

–Not applicable.
[a]$EC_{50}$: The effective concentration required to protect MT-4 cells against HIV-induced cytopathogenicity by 50%.
[b]$CC_{50}$: The cytotoxic concentration of the compound that reduced the normal uninfected MT-4 cell viability by 50%.
[c]SI: selectivity index, ratio $CC_{50}/EC_{50}$ (WT).
[d]The concentration unit is μg/mL.

**Table 2** Anti-HIV-1 activity against mutant strains in MT-4 cells.

| Compd. | $EC_{50}$[a] (nmol/L) | | | | | | |
|---|---|---|---|---|---|---|---|
| | L100I | K103N | Y181C | Y188L | E138K | RES056[b] | F227L + V106A[b] |
| **5h** | 8.2 ± 2.2 | 3.6 ± 0.9 | 9.2 ± 0.8 | 23 ± 6 | 6.5 ± 0.6 | 190 ± 50 | 930 ± 110 |
| **5j** | 12 ± 2 | 3 ± 1 | 13 ± 2 | 17 ± 3 | 6.4 ± 0.1 | 34 ± 4 | 17 ± 4 |
| **6e** | 22 ± 6 | 3.4 ± 0.5 | 11 ± 1 | 50 ± 8 | 5.3 ± 3.3 | 60 ± 7 | ≥16,410 |
| **6i** | 29 ± 0.0 | 7.4 ± 2.1 | 17 ± 5 | 67 ± 16 | 10 ± 2 | 350 ± 80 | ≥3690 |
| **6k** | 4.1 ± 0.5 | 2.3 ± 0.5 | 3 ± 0.2 | 10 ± 3 | 3.5 ± 0.8 | 60 ± 0.0 | 1040 |
| NVP | 460 ± 110 | 3190 ± 3900 | >4000 | >4000 | 57 ± 6 | >4000 | >4000 |
| EFV | 14 ± 0.0 | 30 ± 11 | 1.3 ± 0.1 | 82 ± 7 | 1.5 ± 0.1 | 71 ± 36 | 84 ± 20 |
| ETR | 4.7 ± 2.8 | 1.2 ± 0.1 | 6 ± 1.8 | 12 ± 0.0 | 5.4 ± 0.6 | 15 ± 6 | 10 ± 1 |

[a]$EC_{50}$: The effective concentration required to protect MT-4 cells against viral cytopathicity by 50%.
[b]The double mutant strain (RES056 is referred to K103N/Y181C).

hydrogen bonds and the $\pi-\pi$ stacking effect between the biphenyl group and the groove site of NNIBP. Differently, the tetrahydropyranyl-amino side chain at the C6-position of the compound **5b** pointed towards Pro236 pocket and the aromatic cyanophenyl ring was located close to the entrance channel of RT. The inverted conformations of the two compounds could explain the biological activity different from the more active compounds **5j** and **6k**. The interaction between the less inactive compound **5k** with NNIBP involved no hydrogen bond while keeping the $\pi-\pi$ stacking effect. Therefore, the predicted binding modes of the less active compounds were similar in their conformations, with the substituents (R-) at the C6-position of DATAs protruding to the solvent exposed area instead of the 4-cyanoanaline group. The above analysis suggested the newly designed DATAs improved the positional adaptability, leading to their higher antiviral activity.

Finally, molecular dynamic (MD) simulations were carried out to examine the binding stability of the active compounds **5j** and **6k** with RT using GROMACS 5.0[35]. General procedures about the MD are described in the supporting material. The initial and final binding modes of compound **5j** and **6k** with the low root-mean square deviation (RMSD) between the energy-minimized average structures were obtained. Both compounds (**5j** and **6k**) bound with HIV-1 RT *via* the biphenyl moiety accommodating stability in the hydrophobic binding pocket formed by Phe227, Tyr181 and Trp229 (Fig. 5). Analysis diagram of MD trajectories for ligand **5j** (left) and ligand **6k** (right) in complex with WT HIV-RT was also provided in the supporting material with a normal distribution of RMSD values for both the protein and ligands **5j** and **6k** (Supporting Information Fig. S2).

## 3. Conclusions

In summary, a series of novel DATAs were designed and synthesized with the purpose to improve the positional adaptability with HIV-1 RT. These new target molecules shared the following three main structure features: various side chains on 6-position to occupy the entrance channel, 4-cyanobiphenyl on 4-position to strength the hydrophobic interaction with the tunnel site and 4-cyanoaniline on the 2-position of DATA to occupy the solvent–protein interfere. All the target compounds could inhibit HIV-1 in MT-4 cells with $EC_{50}$ values in the nanomolar range, among which the two most potent compounds **5j** and **6k** showed single-digit nanomolar activity comparable to ETR. These two compounds also showed potency against most of the HIV-1 mutant strains, among which **5j** also exhibited improved activity against the double mutants. The enzymatic assay supported that these new DATAs could specifically target HIV-1 RT NNIBP instead of RNase H. Molecular simulation research also predicted the binding modes for the compounds, explaining their biological activity. The PK and metabolic studies provided future directions for structural optimizations of DATAs.

## 4. Experimental

### 4.1. Chemistry

Chemical reagents and solvents were purchased from the commercial sources as the analytical grade, which were used without further purification. All air-sensitive reactions were run under a nitrogen atmosphere. All solvents were purchased from Sinopharm Group Co. Company (Shanghai, China). All reagents were purchased from Bide Pharmatech Ltd. Company (Shanghai, China), except for $PdCl_2$ was purchased from Energy Chemical Ltd. Company (Shanghai, China). All the reactions were monitored by TLC on the re-coated silica gel G (HSGF254) plates purchased from Yantai Jiangyou Silica Gel Development Co. Ltd. (Yantai, China) at 254 nm under a UV lamp from Shanghai Hele Analytical Instrument Co., Ltd. (Shanghai, China) using ethyl

**Table 3** Inhibitory activity of the target compounds against WT HIV-1 RT.[a]

| Compd. | RT $IC_{50}$[b] (μg/mL) | RNase H $IC_{50}$[d] (μg/mL) | Compd. | $IC_{50}$ (μg/mL) | RNase H $IC_{50}$ (μg/mL) |
|---|---|---|---|---|---|
| **5a** | 0.047 ± 0.003 | >600 | **6d** | 0.128 ± 0.007 | >600 |
| **5b** | 0.136 ± 0.011 | >600 | **6e** | 0.055 ± 0.003 | >600 |
| **5c** | 0.112 ± 0.003 | >600 | **6f** | 0.138 ± 0.131 | >600 |
| **5d** | 0.149 ± 0.004 | >600 | **6g** | 0.069 ± 0.002 | >600 |
| **5e** | 0.098 ± 0.004 | 332 ± 60 | **6h** | 0.171 ± 0.018 | >600 |
| **5f** | 0.242 ± 0.020 | >600 | **6i** | 0.117 ± 0.012 | >600 |
| **5g** | 0.145 ± 0.009 | >600 | **6j** | 0.081 ± 0.003 | >600 |
| **5h** | 0.081 ± 0.003 | >417 | **6k** | 0.052 ± 0.012 | >600 |
| **5i** | 0.146 ± 0.016 | 259 ± 20 | **6l** | 0.115 ± 0.021 | >600 |
| **5j** | 0.096 ± 0.016 | >600 | **6m** | 0.096 ± 0.013 | >543 |
| **5k** | 0.368 ± 0.021 | >600 | **6n** | 0.087 ± 0.008 | >600 |
| **6a** | 0.035 ± 0.008 | >600 | NVP | 0.102 ± 0.026 | ND |
| **6b** | 0.033 ± 0.004 | >600 | EFV | 0.0014 ± 0.0004 | ND |
| **6c** | 0.127 ± 0.026 | >600 | ETR[c] | 0.100 ± 0.000 | ND |
| | | | SGI/DS8000[e] | − | 1.4 ± 0.1 |

−Not applicable.
[a]Data represent the mean values of at least two separate experiments.
[b]$IC_{50}$: inhibitory concentration of test compound required to inhibit biotin deoxyuridine triphosphate (biotin-dUTP) incorporation into WT HIV-1 RT by 50%.
[c]The data were obtained from the same laboratory with the same method.
[d]Data represent the mean values of four times of separate experiments.
[e]Reference compound for HIV-1 RT RNase H inhibitory activity.

**Table 4** Physicochemical parameters of **5a**, **5j**, **6e**, **6i** and **6k**.

| Compd. | Kinetic aqueous solubility (μg/mL, μmol/L)[a] | | | | *c*Log*P*[c] | PSA (Å$^2$)[c] |
|---|---|---|---|---|---|---|
| | pH 7.4 | pH 7.0 | pH 2.0 | FaSSIF[b] | | |
| **5h** | <0.786, <1.56 | <0.786, <1.56 | 3.45, 6.85 | 14.7, 29.2 | 6.217 | 217.635 |
| **5j** | <0.853, <1.56 | <0.853, <1.56 | 6.58, 12.1 | 41.6, 76.2 | 6.680 | 196.656 |
| **6e** | <0.806, <1.56 | <0.806, <1.56 | 12.1, 23.4 | 60.5, 117 | 7.103 | 193.296 |
| **6i** | <0.804, <1.56 | <0.804, <1.56 | 77.3, 150 | 60.6, 117 | 6.725 | 215.847 |
| **6k** | <0.784, <1.56 | <0.784, <1.56 | 53.7, 104 | 53.4, 104 | 6.106 | 228.098 |
| ETR | <1, <2.30 | <1, 2.30 | 127, 291 | 13.2, 30.3 | 5.224 | 233.983 |

[a]Measured by HPLC.
[b]FaSSIF: fasted state simulated intestinal fluid.
[c]Predicted by the software of Sybyl 2.0.

acetate/*n*-hexane as the eluent. Flash column chromatography was performed on glass column packed with silica gel (200−300 mesh) purchased from Qingdao Marine Chemical Plant (Qingdao, China) using ethyl acetate/*n*-hexane as the eluent. Melting points were measured on an SGW X-1 microscopic melting point apparatus from Shanghai Precision Scientific Instrument Co., Ltd. (Shanghai, China). $^1$H NMR and $^{13}$C NMR spectra were recorded on a Bruker AV400 MHz spectrometer (Zurich, Switzerland) in DMSO-$d_6$. Chemical shifts were reported in $\delta$ (ppm) units relative to the internal standard tetramethylsilane (TMS). Mass spectra and HRMS were obtained on a Waters Quattro Micromass instrument (Manchester, England) and Bruker Compact instrument (Bremen, German), respectively, using electrospray ionization (ESI) techniques. The purities of the target compounds were ≥95%, measured by HPLC, performed on an Agilent 1200 HPLC system (Waldbronn, German) with UV detector (Waldbronn) and Agilent Eclipse Plus C18 column (Waldbronn, 150 mm × 4.6 mm, 5 mm), eluting with a mixture of solvents $H_2O$ (A) and $CH_3CN$ (B) from VA:VB = 90:10 to 10:90. Peaks were detected at $\lambda$ = 254 nm with a flow rate of 1.0 mL/min.

#### *4.1.1. Preparation of 4′-((4-chloro-6-((4-cyanophenyl)amino)-1,3,5-triazin-2-yl)oxy)-3′,5′-dimethyl-[1,1′-biphenyl]-4-carbonitrile (**4a**)*

To a solution of compound **3a** (2.23 g, 10.0 mmol) and NaH (1.1 equiv) in dry tetrahydrofuran (THF, 20 mL) compound **3b** (1.0 equiv.) was slowly added at 0 °C. The mixture warmed to room temperature and stirred for 3 h. Then the mixture was poured into crushed ice, which was filtered to give a filter cake. The crude product was dried before being recrystallized from ethyl acetate/petroleum ether (EA/PE) to afford pure **4a**. Yield 67%; white solid; m.p. 242−244 °C (EA/PE); $^1$H NMR (400 MHz, DMSO-$d_6$) $\delta$: 11.13 (m, 1H, NH), 8.01−7.83 (m, 6H, ArH), 7.61 (s, 4H, ArH), 2.20 (s, 6H, $CH_3$ × 2); $^{13}$C NMR (101 MHz, DMSO-$d_6$) $\delta$: 163.36 ($N_2$=C−O), 149.82 ($N_2$=C−Cl), 144.42 ($N_2$=C−NH), 142.70 (ArC), 136.58 (ArC), 133.31 (ArC), 131.29 (ArC), 128.00 (ArC),

**Table 5** Inhibition effects of **5j** on cytochrome P450 (including CYP isozymes: CYP1A2, CYP2C9, CYP2C19, CYP2D6 and CYP3A4M).

| CYP isozyme | Standard inhibitor | $IC_{50}$ (μmol/L) | $IC_{50}$ acceptance range (μmol/L) | Pass/No pass | Compd. | $IC_{50}$ (μmol/L) |
|---|---|---|---|---|---|---|
| 1A2 | α-Naphthoflavone | 0.290 | 0.125–0.448 | Pass | **5j** | >50.0 |
| 2C9 | Sulfaphenazole | 0.748 | 0.333–0.750 | Pass | **5j** | 32.9 |
| 2C19 | (+)-*N*-3-benzylnirvanol | 0.210 | 0.0928–0.333 | Pass | **5j** | >50.0 |
| 2D6 | Quinidine | 0.143 | 0.0928–0.226 | Pass | **5j** | >50.0 |
| 3A4M | Ketoconazole | 0.0410 | 0.0303–0.0928 | Pass | **5j** | >50.0 |

**Table 6** Plasma protein binding rate of compound **5j**.

| Compd.[a] | Protein-binding rate (%) | | Recovery rate (%) | |
|---|---|---|---|---|
| | Human plasma protein | Rat plasma protein | Human plasma protein | Rat plasma protein |
| **5j** | 99.95 | 99.96 | 84.9 | 99.5 |
| Warfarin (control drug) | 98.8 | 99.4 | 86. | 99.0 |

[a]The test concentrations of compound **5j** and warfarin are 2 μmol/L.

120.68 (ArC), 119.33(C≡N), 110.52 (ArC), 16.61 ($CH_3$); HRMS Calcd. for $C_{25}H_{17}ClN_6O$ $[M+Na]^+$: 475.1045, Found: 475.1045.

*4.1.2. Preparation of 4′-((4-chloro-6-((4-cyanophenyl)amino)-1,3,5-triazin-2-yl)amino)-3′,5′-dimethyl-[1,1′-biphenyl]-4-carbonitrile (**4b**)*

To a solution of compound **3a** (2.23 g, 10.0 mmol) and diisopropyl ethylamine (DIPEA, 1.1 equiv) in dry THF (20 mL), compound **3b-1** (1.0 equiv.) was slowly added at room temperature. Then the mixture refluxed for 3 h. The mixture cooled to room temperature and poured into crushed ice, filtered and the filter cake was dried. The crude product was then recrystallized from EA/PE to afford **4b**. Yield 69%; white solid; m.p. 269–270 °C (EA/PE); $^1$H NMR (400 MHz, DMSO-$d_6$) δ: 10.57 (m, 1H, NH), 9.87 (m, 1H, NH), 8.06−7.53 (m, 10H, ArH), 2.26 (s, 6H, $CH_3$ × 2); $^{13}$C NMR (101 MHz, DMSO-$d_6$) δ: 169.54 ($N_2$=C−NH), 169.03 ($N_2$=C−Cl), 165.47 ($N_2$=C−NH), 164.39 (ArC), 164.16 (ArC), 144.72 (ArC), 143.82 (ArC), 137.33 (ArC), 137.00 (ArC), 136.94 (ArC), 136.02 (ArC), 135.71 (ArC), 133.55 (ArC), 133.32 (ArC), 133.25 (ArC), 133.12 (ArC), 127.98 (ArC), 127.12 (ArC), 120.41 (ArC), 120.41 (ArC), 119.50 (C≡N), 119.37 (C≡N), 110.47 (ArC), 18.88 ($CH_3$), 14.56; HRMS Calcd. for $C_{25}H_{18}ClN_7$ $[M+Na]^+$: 474.1204, Found: 474.1213.

*4.1.3. General procedure for preparing the target compounds **5a−5k** and **6a−6n***

To a suspension of **14** or **15** (0.50 mmol) and DIPEA (2.2 equiv) in THF (10 mL) were added with various substituted amines (1.0 equiv.). The reaction mixtures were then refluxed until the TLC monitoring test show the completion. The reaction mixtures were then concentrated and extracted with EA (10 mL × 3). The combined extracts were dried over anhydrous $Na_2SO_4$ and concentrated under *vacuum* to give the crude products, which were purified by flash column chromatography and recrystallized from EA/PE to afford the target compounds **5a−5k** or **6a−6n**.

**Table 7** The pharmacokinetic profile of **5j**.[a]

| Subject | $t_{1/2}$ (h) | $T_{max}$ (h) | $C_{max}$ (ng/mL) | $AUC_{0-t}$ (h·ng/mL) | $AUC_{0-\infty}$ (h·ng/mL) | CL (mL/min·kg) | *F* (%) |
|---|---|---|---|---|---|---|---|
| **5j** (i.v., 1 mg/kg) | 0.734 ± 0.174 | − | − | 6647 ± 795 | 6662 ± 809 | 5.06 ± 0.658 | − |
| **5j** (*p.o.*, 20 mg/kg) | ND | 13.3 ± 9.24 | 43.23 ± 39.8 | 322 ± 176 | − | − | 0.485 |

−Not applicable.
[a]PK parameters (mean ± SD, $n$ = 3).

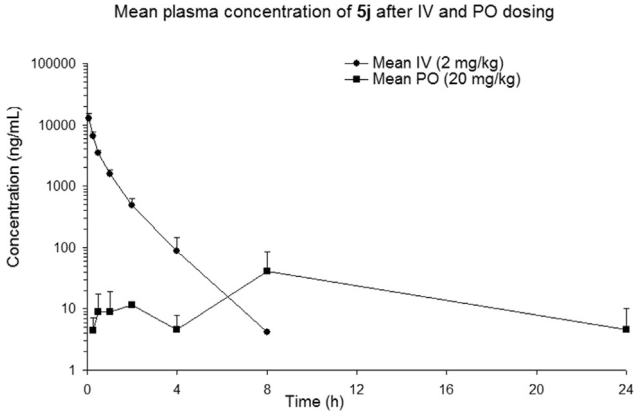


**Figure 2** Mean plasma concentration−time profiles of compound **5j** in rats following oral or intravenous administration.

*4.1.3.1. Methyl (4-((4′-cyano-3,5-dimethyl-[1,1′-biphenyl]-4-yl)oxy)-6-((4-cyanophenyl)-amino)-1,3,5-triazin-2-yl) glycinate (**5a**).* Yield 70%; white solid; m.p. 192–194 °C (EA/PE); IR: υ 3267, 2216, 1717, 1582, 1491 $cm^{-1}$; $^1$H NMR (400 MHz, DMSO-$d_6$) δ: 10.15 (m, 1H, NH), 8.26 (s, 1H, NH), 8.26−7.56 (m, 10H), 3.97 (m, 2H, $CH_2$), 3.61 (m, 3H, $OCH_3$), 2.17 (m, 6H, $CH_3$ × 2); $^{13}$C NMR (101 MHz, DMSO-$d_6$) δ: 170.84 (C=O), 169.96 ($N_2$=C−O), 167.84 ($N_2$=C−NH), 165.69 ($N_2$=C−NH), 150.35 (ArC), 144.62 (ArC), 144.37 (ArC), 135.84 (ArC), 133.23 (ArC), 131.48 (ArC), 127.86 (ArC), 127.56 (ArC), 120.05 (ArC), 119.69 (C≡N), 119.37 (C≡N), 110.34 (ArC), 52.32 ($COCH_2NH$), 52.12

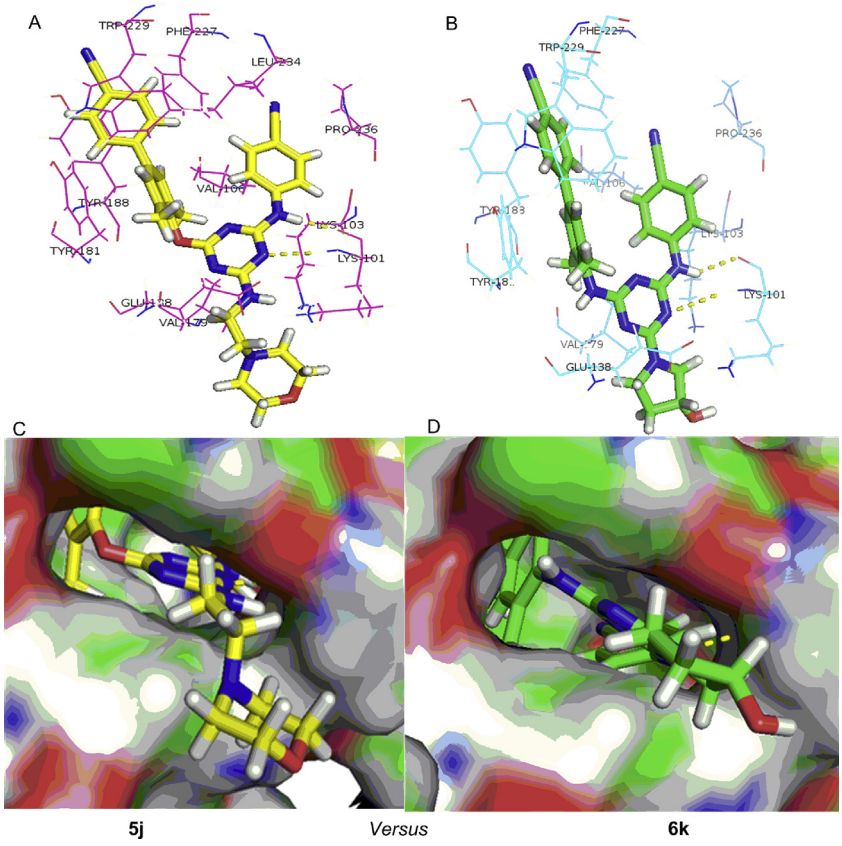


**Figure 3** The predicted binding modes of **5j** (A) and **6k** (B) with the HIV-1 WT RT NNIBP. Hydrogen bonds between inhibitors and amino acid residues are indicated with yellow dashed lines. (C) and (D) The 6-side chains of DATAs fitted well in the narrow entrance channel of NNIBP, respectively.

($COCH_2NH$), 42.54 ($OCH_3$), 16.65 ($CH_3$); HRMS Calcd. for $C_{28}H_{23}N_7O_3$ $[M+Na]^+$: 528.1755, Found: 528.1751.

*4.1.3.2. 4′-((4-((4-Cyanophenyl)amino)-6-((tetrahydro-2H-pyran-4-yl)amino)-1,3,5-triazin-2-yl)oxy)-3′,5′-dimethyl-[1,1′-biphenyl]-4-carbonitrile (**5b**).* Yield 66%; white solid; m.p.>300 °C (EA/PE); IR: $\upsilon$ 3258, 2219, 1602, 1574, 1488 $cm^{-1}$; $^1H$ NMR (400 MHz, DMSO-$d_6$) $\delta$: 10.02 (m, 1H, NH), 8.05−7.50 (m, 11H, ArH), 3.90 (m, 3H, CH, $CH_2$), 3.41 (m, 2H, $CH_2$), 2.18 (s, 6H, $CH_3 \times 2$), 1.78 (m, 2H, $CH_2$), 1.53 (m 2H, $CH_2$); $^{13}C$ NMR (101 MHz, DMSO-$d_6$) $\delta$: 170.23 ($N_2$═C−O), 169.95 ($N_2$═C−NH), 166.71 ($N_2$═C−NH), 165.88 (ArC), 165.42 (ArC), 150.48 (ArC), 144.65 (ArC), 135.75 (ArC), 133.28 (ArC), 133.23 (ArC), 133.12 (ArC), 131.57 (ArC), 127.86 (ArC), 127.76 (ArC), 127.62 (ArC), 119.97 (ArC), 119.74 (C≡N), 119.36 (C≡N), 110.31 (ArC), 103.96 (ArC), 66.53 ($OCH_2$), 47.41 (CHNH), 32.68 ($CH_2$), 16.74 ($CH_3$); HRMS Calcd. for $C_{30}H_{27}N_7O_2$ $[M+Na]^+$: 540.2118, Found: 540.2104.

*4.1.3.3. 4′-((4-((4-Cyanophenyl)amino)-6-(((tetrahydrofuran-3-yl)methyl)amino)-1,3,5-triazin-2-yl)oxy)-3′,5′-dimethyl-[1,1′-biphenyl]-4-carbonitrile (**5c**).* Yield 72%; white solid; m.p. 195−197 °C (EA/PE); IR: $\upsilon$ 3386, 2222, 2213, 1571, 1506, 1398 $cm^{-1}$; $^1H$ NMR (400 MHz, DMSO-$d_6$) $\delta$: 10.05 (m, 1H, NH), 7.78 (m, 11H, ArH), 3.67 (m, 4H, $CH_2$), 3.16 (m, 2H, $CH_2$), 2.35−1.88 (m, 7H, $CH_3 \times 2$, CH), 1.97 (m, 2H, $CH_2$); $^{13}C$ NMR (101 MHz, DMSO-$d_6$) $\delta$: 169.87 ($N_2$═C−O), 167.58 ($N_2$═C−NH), 165.86 ($N_2$═C−NH), 150.43 (ArC), 144.64 (ArC), 135.75 (ArC), 133.26 (ArC), 131.58 (ArC), 127.89 (ArC), 127.77 (ArC), 120.02 (ArC), 119.37 (C≡N), 110.31 (ArC), 70.93 ($OCH_2$), 67.23 ($OCH_2$), 44.00 ($NCH_2$), 43.43 ($CH_2$), 29.94 (CH), 16.74 ($CH_3$); HRMS Calcd. for $C_{30}H_{27}N_7O_2$ $[M+Na]^+$: 540.2118, Found: 540.2113.

*4.1.3.4. Methyl (4-((4′-cyano-3,5-dimethyl-[1,1′-biphenyl]-4-yl)oxy)-6-((4-cyanophenyl)-amino)-1,3,5-triazin-2-yl)-L-prolinate (**5d**).* Yield 72%; white solid; m.p. 187−189 °C (EA/PE); IR: $\upsilon$ 3318, 2225, 1745, 1575, 1507 $cm^{-1}$; $^1H$ NMR (400 MHz, DMSO-$d_6$) $\delta$: 10.15 (m, 1H, NH), 8.13−7.33 (m, 10H, ArH), 4.71−4.22 (m, 1H, CH), 3.63 (m, 3H, $OCH_3$), 3.47 (s, 2H, $CH_2$), 2.41−1.84 (m, 10H, $CH_3 \times 2$, $CH_2$); $^{13}C$ NMR (101 MHz, DMSO-$d_6$) $\delta$: 173.15 (C═O), 172.73 ($N_2$═C−O), 169.83 ($N_2$═C−NH), 169.43 ($N_2$═C−NH), 165.64 (ArC), 165.03 (ArC), 164.93 (ArC), 164.75 (ArC), 144.58 (ArC), 144.31 (ArC), 133.30 (ArC), 133.06 (ArC), 131.44 (ArC), 127.84 (ArC), 127.51 (ArC), 120.05 (ArC), 119.38 (C≡N), 110.28 (ArC), 104.17 (ArC), 59.06 (NCHC═O), 52.56 ($CH_3$), 52.27 ($CH_2$), 47.37 ($CH_2$), 29.95 ($CH_2$), 23.82 ($CH_2$), 16.80 ($CH_3$), 16.55 ($CH_3$); HRMS Calcd. for $C_{31}H_{27}N_7O_3$ $[M+H]^+$: 546.2248, Found: 546.2249.

*4.1.3.5. 4′-((4-((4-Cyanophenyl)amino)-6-morpholino-1,3,5-triazin-2-yl)oxy)-3′,5′-dimeth-yl-[1,1′-biphenyl]-4-carbonitrile (**5e**).* Yield 73%; white solid; m.p.>300 °C (EA/PE); IR: $\upsilon$ 3288, 2222, 1576, 1504, 1405 $cm^{-1}$; $^1H$ NMR (400 MHz, DMSO-$d_6$) $\delta$:

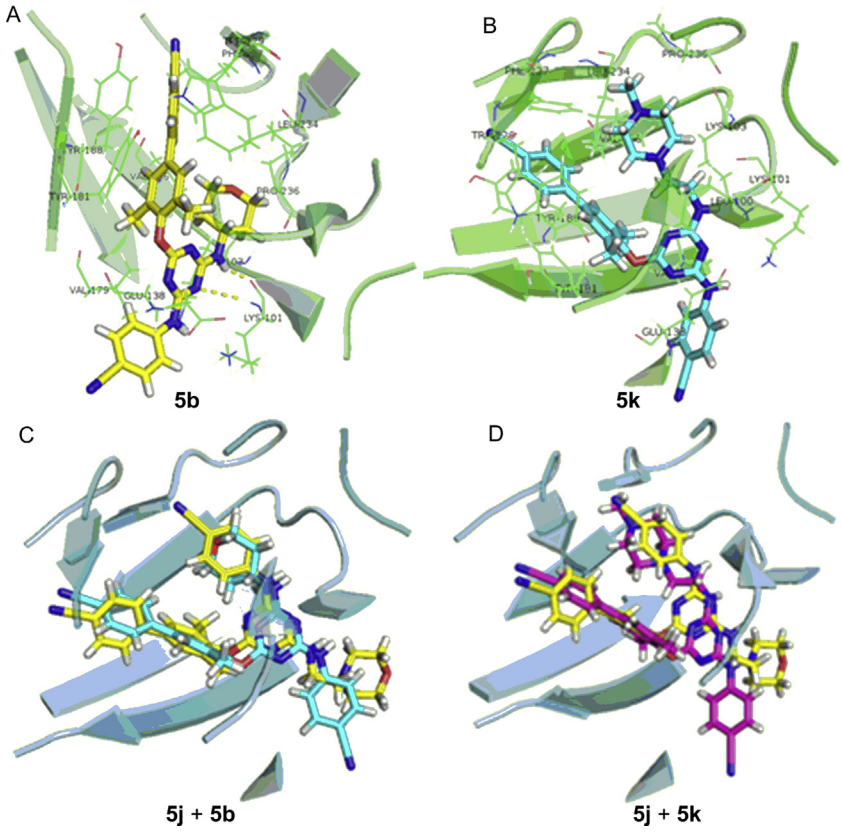


**Figure 4** Docking modes of **5b** (yellow) and **5k** (blue) in RT NNIBP (A) and (B) and the superpositions of **5j** (yellow) with **5b** (cyanide blue) or **5k** (purple) in RT NNIBP (C) and (D).

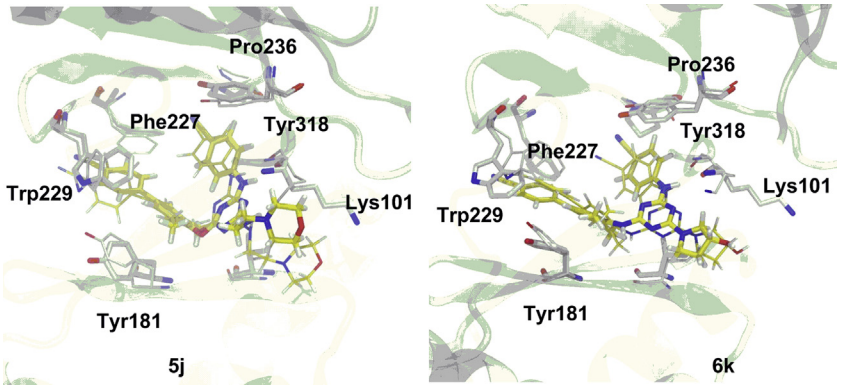


**Figure 5** The initial (thinner stick) and final (thicker stick) binding modes for ligand **5j** (left) and **6k** (right) into NNIBP (2ZD1) of HIV *via* molecular dynamics simulations.

10.12 (s, 1H, NH), 7.94 (s, 4H, ArH), 7.66 (m, 6H, ArH), 3.73 (m, 8H, $CH_2$), 2.19 (s, 6H, $CH_3 \times 2$); $^{13}$C NMR (101 MHz, DMSO-$d_6$) $\delta$: 170.20 ($N_2$=C−O), 166.36 ($N_2$=C−NH), 165.55 ($N_2$=C−N), 150.43 (ArC), 144.49 (ArC), 142.70 (ArC), 135.73 (ArC), 133.26 (ArC), 131.53 (ArC), 131.41 (ArC), 127.87 (ArC), 120.11 (ArC), 119.67 (C≡N), 119.38 (C≡N), 110.33 (ArC), 104.09 (ArC), 66.24 ($CH_2$), 44.26 ($CH_2$), 43.99 ($CH_2$), 30.90 ($CH_2$), 16.69 ($CH_3$); HRMS Calcd. for $C_{29}H_{25}N_7O_2$ $[M+Na]^+$: 526.1962, Found: 526.1979.

*4.1.3.6. 4′-((4-((4-Cyanophenyl)amino)-6-(piperazin-1-yl)-1,3,5-triazin-2-yl)oxy)-3′,5′-dimethyl-[1,1′-biphenyl]-4-carbonitrile (**5f**).* Yield 72%; white solid; m.p. 267−269 °C (EA/PE); IR: $\upsilon$ 3311, 2223, 1574, 1504, 1404 cm$^{-1}$; $^1$H NMR (400 MHz, DMSO-$d_6$) $\delta$: 10.11 (m, 1H, NH), 8.02−7.48 (m, 10H, ArH), 4.11−3.37 (m, 6H, $CH_2$), 2.75 (m, 3H, $CH_2$, NH), 2.19 (s, 6H, $CH_3 \times 2$); $^{13}$C NMR (101 MHz, DMSO-$d_6$) $\delta$: 170.18 ($N_2$=C−O), 166.09 ($N_2$=C−NH), 165.54 ($N_2$=C−N), 150.49 (ArC), 144.56 (ArC), 135.67 (ArC), 133.26 (ArC), 131.54 (ArC), 127.79 (ArC), 120.01 (ArC), 119.70 (C≡N), 119.39 (C≡N), 110.32 (ArC), 103.96 (ArC), 70.26 ($CH_2$), 45.78 ($CH_2$), 45.11 ($CH_2$), 44.82 ($CH_2$), 30.90 ($CH_2$), 16.79 ($CH_3$); HRMS Calcd. for $C_{29}H_{26}N_8O$ $[M+H]^+$: 503.2302, Found: 503.2321.

*4.1.3.7. 4′-((4-((4-Cyanophenyl)amino)-6-(2-(hydroxymethyl) pyrrolidin-1-yl)-1,3,5-triazin-2-yl)oxy)-3′,5′-dimethyl-[1,1′-*

*biphenyl]-4-carbonitrile (**5g**).* Yield 52%; white solid; m.p. 235–237 °C (EA/PE); IR: $\upsilon$ 3431, 2224, 1573, 1496, 1396 $cm^{-1}$; $^1H$ NMR (400 MHz, DMSO-$d_6$) $\delta$: 10.02 (m, 1H, NH), 7.97−7.32 (m, 10H, ArH), 4.73 (m, 1H, OH), 4.10 (m, 1H, NCH), 3.55 (m, 4H, $CH_2$), 2.23−1.70 (m, 10H, $CH_2$, $CH_3$ × 2). $^{13}C$ NMR (101 MHz, DMSO-$d_6$) $\delta$: 169.73 ($N_2$=C−O), 165.24 ($N_2$=C−NH), 165.09 ($N_2$=C−N), 164.99 (ArC), 164.87 (ArC), 150.51 (ArC), 144.68 (ArC), 135.67 (ArC), 133.29 (ArC), 133.17 (ArC), 131.55 (ArC), 127.88 (ArC), 127.67 (ArC), 119.83 (ArC), 119.38 (C≡N), 119.08 (C≡N), 110.28 (ArC), 103.83 (ArC), 70.24 (CH), 61.15 ($CH_2$), 59.45 ($CH_2$), 47.79 ($CH_2$), 47.63 ($CH_2$), 27.78 ($CH_2$), 23.07 ($CH_2$), 16.75 ($CH_3$); HRMS Calcd. for $C_{30}H_{27}N_7O_2$ $[M+Na]^+$: 540.2118, Found: 540.2110.

*4.1.3.8. 4′-((4-((4-Cyanophenyl)amino)-6-(3-hydroxypyrrolidin-1-yl)-1,3,5-triazin-2-yl)-oxy)-3′,5′-dimethyl-[1,1′-biphenyl]-4-carbonitrile (**5h**).* Yield 67%; white solid; m.p. 204–206 °C (EA/PE); IR: $\upsilon$ 3191, 2226, 1576, 1489, 1410 $cm^{-1}$; $^1H$ NMR (400 MHz, DMSO-$d_6$) $\delta$: 10.04 (m, 1H, NH), 7.93−7.57 (m, 10H, ArH), 5.04 (m, 1H, OH), 4.42−4.26 (m, 1H, OCH), 3.78−3.43 (m, 4H, $CH_2$), 2.34−1.69 (m, 8H, $CH_2$, $CH_3$ × 2); $^{13}C$ NMR (101 MHz, DMSO-$d_6$) $\delta$: 169.74 ($N_2$=C−O), 165.16 ($N_2$=C−NH), 164.91 ($N_2$=C−N), 150.53 (ArC), 144.67 (ArC), 135.64 (ArC), 133.22 (ArC), 131.57 (ArC), 127.77 (ArC), 119.82 (C≡N), 119.38 (C≡N), 110.30 (ArC), 103.80 (ArC), 70.23 ($CH_2$), 69.18 ($CH_2$), 55.12 (CH), 45.03 ($CH_2$), 44.76 ($CH_2$), 33.53 ($CH_2$), 16.78 ($CH_3$); HRMS Calcd. for $C_{29}H_{25}N_7O_2$ $[M+Na]^+$: 526.1962, Found: 526.1966.

*4.1.3.9. 4′-((4-((4-Cyanophenyl)amino)-6-(4-hydroxypiperidin-1-yl)-1,3,5-triazin-2-yl)-oxy)-3′,5′-dimethyl-[1,1′-biphenyl]-4-carbonitrile (**5i**).* Yield 71%; white solid; m.p. 228–240 °C (EA/PE); IR: $\upsilon$ 3285, 2227, 1576, 1492, 1407 $cm^{-1}$; $^1H$ NMR (400 MHz, DMSO-$d_6$) $\delta$: 10.06 (s, 1H, NH), 7.93−7.57 (m, 10H, ArH), 4.80 (s, 1H, OH), 4.13 (m, 3H, $CH_2$, CH), 3.77 (s, 1H, $CH_2$), 3.42 (s, 1H, $CH_2$), 1.77 (m, 10H, $CH_2$, $CH_3$ × 2); $^{13}C$ NMR (101 MHz, DMSO-$d_6$) $\delta$: 170.27 ($N_2$=C−O), 165.91 ($N_2$=C−NH), 165.63 ($N_2$=C−N), 150.51 (ArC), 144.57 (ArC), 135.67 (ArC), 133.24 (ArC), 131.54 (ArC), 127.87 (ArC), 127.67 (ArC), 127.32 (ArC), 119.97 (ArC), 119.83 (C≡N), 119.38 (C≡N), 110.31 (ArC), 103.93 (ArC), 65.99 ($NCH_2$), 41.41 ($NCH_2$), 41.09 ($OCH_2$), 34.27 ($OCH_2$), 16.68 ($CH_3$); HRMS Calcd. for $C_{30}H_{27}N_7O_2$ $[M+Na]^+$: 540.2118, Found: 540.2110.

*4.1.3.10. 4′-((4-((4-Cyanophenyl)amino)-6-((2-morpholinoethyl)amino)-1,3,5-triazin-2-yl)-oxy)-3′,5′-dimethyl-[1,1′-biphenyl]-4-carbonitrile (**5j**).* Yield 73%; white solid; m.p. 259−261 °C (EA/PE); IR: $\upsilon$ 3261, 2222, 1606, 1583, 1494 $cm^{-1}$; $^1H$ NMR (400 MHz, DMSO-$d_6$) $\delta$: 10.06 (m, 1H, NH), 7.98−7.49 (m, 11H, ArH), 3.56 (s, 2H, $CH_2$), 3.42 (s, 3H, $CH_2$), 3.24 (d, $J$ = 5.1 Hz, 1H, $CH_2$), 2.47 (s, 1H, $CH_2$), 2.39 (s, 2H, $CH_2$), 2.32 (s, 1H, $CH_2$), 2.20 (m, 8H, $CH_3$ × 2, $CH_2$); $^{13}C$ NMR (101 MHz, DMSO-$d_6$) $\delta$: 170.15 ($N_2$=C−O), 169.83 ($N_2$=C−NH), 167.45 ($N_2$=C−N), 165.90 (ArC), 165.52 (ArC), 144.74 (ArC), 144.63 (ArC), 135.74 (ArC), 135.52 (ArC), 133.25 (ArC), 131.54 (ArC), 127.82 (ArC), 127.54 (ArC), 119.90 (ArC), 119.37 (C≡N), 110.30 (ArC), 66.62 ($NCH_2$), 57.56 ($NCH_2$), 53.68 ($NCH_2$), 38.31 ($OCH_2$), 37.59 ($OCH_2$), 16.71 ($CH_3$); HRMS Calcd. for $C_{31}H_{30}N_8O_2$ $[M+H]^+$: 547.2564, Found: 547.2568.

*4.1.3.11. 4′-((4-((4-Cyanophenyl)amino)-6-((2-(4-methylpiperazin-1-yl)ethyl)amino)-1,3,5-triazin-2-yl)oxy)-3′,5′-dimethyl-[1,1′-biphenyl]-4-carbonitrile (**5k**).* Yield 72%; white solid; m.p. 190–192 °C (EA/PE); IR: $\upsilon$ 2939, 2225, 1575, 1507, 1393 $cm^{-1}$; $^1H$ NMR (400 MHz, DMSO-$d_6$) $\delta$: 10.08 (m, 1H, NH), 7.92−7.55 (m, 10H, ArH), 3.20 (s, 3H, $NCH_3$), 2.48–2.01 (m, 18H, $CH_2$, $CH_3$ × 2); $^{13}C$ NMR (101 MHz, DMSO-$d_6$) $\delta$: 170.15 ($N_2$=C−O), 169.81 ($N_2$=C−N), 167.42 ($N_2$=C−N), 144.65 (ArC), 135.7 2(ArC), 133.31 (ArC), 133.25 (ArC), 133.19 (ArC), 131.52 (ArC), 127.90 (ArC), 127.82 (ArC), 127.77 (ArC), 127.55 (ArC), 119.90 (C≡N), 119.38 (C≡N), 110.27 (ArC), 70.22 ($NCH_2$), 57.05 ($NCH_2$), 55.02 ($NCH_2$), 52.80 ($NCH_2$), 45.98 ($NCH_2$), 38.59 ($NCH_3$), 16.71 ($CH_3$); HRMS Calcd. for $C_{32}H_{33}N_9O$ $[M+H]^+$: 560.2881, Found: 560.2888.

*4.1.3.12. 4′-((4-((4-Cyanophenyl)amino)-6-(cyclopropylamino)-1,3,5-triazin-2-yl)amino)-3′,5′-dimethyl-[1,1′-biphenyl]-4-carbonitrile (**6a**).* Yield 71%; white solid; m.p. 262–264 °C (EA/PE); IR: $\upsilon$ 3419, 2218, 1567, 1472, 1412 $cm^{-1}$; $^1H$ NMR (400 MHz, DMSO-$d_6$) $\delta$: 9.63−9.37 (m, 1H, NH), 8.78−8.45 (m, 1H, NH), 8.17−7.91 (m, 6H, ArH), 7.29−7.71 (m, 5H, ArH), 2.76 (s, 1H, CH), 2.26 (s, 6H, $CH_3$ × 2), 0.73−0.48 (m, 4H, $CH_2$ × 2). $^{13}C$ NMR (101 MHz, DMSO-$d_6$) $\delta$: 169.13 ($N_2$=C−NH), 167.65 ($N_2$=C−NH), 165.38 ($N_2$=C−NH), 145.75 (ArC), 144.97 (ArC), 137.54 (ArC), 136.43 (ArC), 133.28 (ArC), 132.92 (ArC), 127.83 (ArC), 126.83 (ArC), 119.73 (C≡N), 110.22 (ArC), 102.71 (ArC), 24.01 (CH), 18.88 ($CH_3$), 6.84 ($CH_2$), 6.52 ($CH_2$); HRMS Calcd. for $C_{28}H_{24}N_8$ $[M+H]^+$: 473.2197, Found: 473.2189.

*4.1.3.13. Methyl (4-((4′-cyano-3,5-dimethyl-[1,1′-biphenyl]-4-yl)amino)-6-((4-cyanophenyl)amino)-1,3,5-triazin-2-yl) glycinate (**6b**).* Yield 68%; white solid; m.p. 197–199 °C (EA/PE); IR: $\upsilon$ 3342, 2221, 1721, 1576, 1494 $cm^{-1}$; $^1H$ NMR (400 MHz, DMSO-$d_6$) $\delta$: 9.57 (m, 1H, N*H* ), 8.74−8.58 (m, 1H, NH), 7.78 (m, 11H, ArH), 4.11 (m, 2H, $CH_2$), 3.66 (s, 3H, $OCH_3$), 2.26 (s, 6H, $CH_3$ × 2); $^{13}C$ NMR (101 MHz, DMSO-$d_6$) $\delta$: 171.61 (C=O), 166.40 ($N_2$=C−NH), 165.67 ($N_2$=C−NH), 164.65 ($N_2$=C−NH), 145.55 (ArC), 144.95 (ArC), 137.43 (ArC), 136.51 (ArC), 133.28 (ArC), 132.88 (ArC), 127.86 (ArC), 126.86 (ArC), 120.03 (ArC), 119.42 (C≡N), 110.23 (ArC), 102.97 (ArC), 52.18 ($NHCH_2$), 42.37 ($OCH_3$), 18.96 ($CH_3$); HRMS Calcd. for $C_{28}H_{24}N_8O_2$ $[M+Na]^+$: 527.1914, Found: 527.1913.

*4.1.3.14. 4′-((4-((4-Cyanophenyl)amino)-6-((tetrahydro-2H-pyran-4-yl)amino)-1,3,5-triazin-2-yl)amino)-3′,5′-dimethyl-[1,1′-biphenyl]-4-carbonitrile (**6c**).* Yield 73%; white solid; m.p. 272–274 °C (EA/PE); IR: $\upsilon$ 3354, 2220, 1611, 1569, 1484 $cm^{-1}$; $^1H$ NMR (400 MHz, DMSO-$d_6$) $\delta$: 9.58−9.35 (m, 1H, NH), 8.56 (m, 1H, NH), 8.08−7.71 (m, 7H, ArH), 7.49 (s, 3H, ArH), 7.12 (s, 1H, ArH), 4.14−3.81 (m, 3H, CH, $CH_2$), 3.36 (s, 2H, $CH_2$), 2.26 (s, 6H, $CH_3$ × 2), 1.81 (m, 2H, $CH_2$), 1.53 (m, 2H, $CH_2$); $^{13}C$ NMR (101 MHz, DMSO-$d_6$) $\delta$: 170.80 ($N_2$=C−NH), 165.71 ($N_2$=C−NH), 164.70 ($N_2$=C−NH), 145.71 (ArC), 144.98 (ArC), 137.54 (ArC), 136.42 (ArC), 133.28 (ArC), 132.92 (ArC), 127.83 (ArC), 126.83 (ArC), 120.09 (ArC), 119.41 (C≡N), 110.23 (ArC), 66.75 (NHCH), 60.23 ($OCH_2$), 47.00 ($OCH_2$), 33.22 ($CH_2$), 21.22 ($CH_2$), 19.00 ($CH_3$), 14.55 (CH); HRMS Calcd. for $C_{30}H_{28}N_8O$ $[M+Na]^+$: 539.2278, Found: 539.2278.

*4.1.3.15. 4′-((4-((4-Cyanophenyl)amino)-6-(((tetrahydro-2H-pyran-4-yl)methyl)amino)-1,3,5-triazin-2-yl)amino)-3′,5′-dimethyl-[1,1′-biphenyl]-4-carbonitrile (**6d**).* Yield 70%; white solid; m.p. 222–224 °C (EA/PE); IR: $\upsilon$ 3385, 2220, 1616, 1509, 1473 $cm^{-1}$; $^1H$ NMR (400 MHz, DMSO-$d_6$) $\delta$: 9.56−9.36 (m, 1H,

NH), 8.64−8.45 (m, 1H, NH), 8.00 (m, 6H, ArH), 7.60 (m, 4H, ArH), 7.19 (m, 1H, ArH), 3.77 (m, 2H, $CH_2$), 3.19 (m, 2H, $CH_2$), 2.26 (s, 6H, $CH_3 \times 2$), 1.85 (s, 1H, CH), 1.61 (m, 2H, $CH_2$), 1.22 (s, 2H, $CH_2$); $^{13}C$ NMR (101 MHz, DMSO-$d_6$) $\delta$: 166.62 ($N_2$=C−NH), 166.41 ($N_2$=C−NH), 164.51 ($N_2$=C−NH), 145.73 (ArC), 144.97 (ArC), 137.52 (ArC), 136.38 (ArC), 133.28 (ArC), 132.89 (ArC), 127.83 (ArC), 126.83 (ArC), 120.11 (ArC), 119.41 (C≡N), 110.21 (ArC), 102.60 (ArC), 67.28 ($NHCH_2$), 46.61 ($OCH_2$), 35.11 ($OCH_2$), 31.10 ($CH_2$), 19.00 (CH); HRMS Calcd. for $C_{31}H_{30}N_8O$ $[M+Na]^+$: 553.2435, Found: 553.2422.

*4.1.3.16. 4′-((4-((4-Cyanophenyl)amino)-6-(((tetrahydrofuran-3-yl)methyl)amino)-1,3,5-triazin-2-yl)amino)-3′,5′-dimethyl-[1,1′-biphenyl]-4-carbonitrile (**6e**).* Yield 70%; white solid; m.p. 197–199 °C (EA/PE); IR: $\upsilon$ 3419, 2224, 1614, 1567, 1484 $cm^{-1}$; $^1H$ NMR (400 MHz, DMSO-$d_6$) $\delta$: 9.58−9.51 (m, 1H, NH), 8.58 (m, 1H, NH), 8.17−7.19 (m, 11H, ArH), 3.72−3.2 (m, 4H, $OCH_2$), 3.22 (s, 2H, $NHCH_2$), 2.52 (s, 1H, CH), 2.26 (s, 6H, $CH_3 \times 2$), 1.98 (s, 1H, $CH_2$), 1.64 (s, 1H, $CH_2$); $^{13}C$ NMR (101 MHz, DMSO-$d_6$) $\delta$: 173.79 ($N_2$=C−NH), 165.52 ($N_2$=C−NH), 164.15 ($N_2$=C−NH), 163.85 (ArC), 145.33 (ArC), 144.98 (ArC), 137.33 (ArC), 133.28 (ArC), 132.86 (ArC), 127.85 (ArC), 126.90 (ArC), 119.47 (C≡N), 110.22 (ArC), 103.03 (ArC), 59.05 ($NCH_2$), 52.37 ($OCH_2$), 47.17 ($OCH_2$), 30.23 ($CH_2$), 23.93 (CH), 19.05 ($CH_3$); HRMS Calcd. for $C_{30}H_{28}N_8O$ $[M+H]^+$: 517.2435, Found: 517.2450.

*4.1.3.17. Methyl (4-((4′-cyano-3,5-dimethyl-[1,1′-biphenyl]-4-yl)amino)-6-((4-cyanophenyl)amino)-1,3,5-triazin-2-yl)-L-prolinate (**6f**).* Yield 68%; white solid; m.p. 209–211 °C (EA/PE); IR: $\upsilon$ 2953, 2223, 1740, 1605, 1471 $cm^{-1}$; $^1H$ NMR (400 MHz, DMSO-$d_6$) $\delta$: 9.68−9.46 (m, 1H), 8.69 (m, 1H, NH), 8.11−7.50 (m, 10H, ArH), 4.61−4.07 (m, 1H, CH), 3.70−3.63 (m, 4H, $CH_3$, $CH_2$), 3.27 (s, 1H, $CH_2$), 2.42−1.70 (m, 10H, $CH_3 \times 2$, $CH_2$); $^{13}C$ NMR (101 MHz, DMSO-$d_6$) $\delta$: 173.79 (C=O), 164.51 ($N_2$=C−NH), 164.15 ($N_2$=C−NH), 144.98 ($N_2$=C−N), 137.45 (ArC), 133.28 (ArC), 132.86 (ArC), 127.85 (ArC), 126.90 (ArC), 119.98 (ArC), 119.52 (C≡N), 119.41 (C≡N), 110.22 (ArC), 103.02 (ArC), 52.37 (NCHC=O), 30.23 ($CH_2$), 19.05 ($CH_3$); HRMS Calcd. for $C_{31}H_{28}N_8O_2$ $[M+Na]^+$: 567.2227, Found: 567.2223.

*4.1.3.18. 4′-((4-((4-Cyanophenyl)amino)-6-morpholino-1,3,5-triazin-2-yl)amino)-3′,5′-dimethyl-[1,1′-biphenyl]-4-carbonitrile (**6g**).* Yield 65%; white solid; m.p. 279–281 °C (EA/PE); IR: $\upsilon$ 3411, 2220, 1620, 1574, 1597 $cm^{-1}$; $^1H$ NMR (400 MHz, DMSO-$d_6$) $\delta$: 9.62 (m, 1H, NH), 8.74 (s, 1H, NH), 8.11−7.65 (m, 7H, ArH), 7.50 (m, 3H, ArH), 3.67 (m, 8H, $CH_2$), 2.26 (s, 6H, $CH_3 \times 2$); $^{13}C$ NMR (101 MHz, DMSO-$d_6$) $\delta$: 165.76 ($N_2$=C−NH), 165.34 ($N_2$=C−NH), 164.67 ($N_2$=C−N), 145.39 (ArC), 144.95 (ArC), 137.41 (ArC), 136.53 (ArC), 133.27 (ArC), 132.97 (ArC), 127.84 (ArC), 126.86 (ArC), 119.91 (ArC), 119.46 (C≡N), 110.26 (ArC), 102.92 (ArC), 66.47 ($NCH_2$), 43.84 ($OCH_2$), 19.04 ($CH_3$); HRMS Calcd. for $C_{29}H_{26}N_8O$ $[M+H]^+$: 503.2302, Found: 503.2291.

*4.1.3.19. 4′-((4-((4-Cyanophenyl)amino)-6-(piperazin-1-yl)-1,3,5-triazin-2-yl)amino)-3′,5′-dimethyl-[1,1′-biphenyl]-4-carbonitrile (**6h**).* Yield 69%; white solid; m.p. 209–211 °C (EA/PE); IR: $\upsilon$ 3329, 2219, 1612, 1568, 1482 $cm^{-1}$; $^1H$ NMR (400 MHz, DMSO-$d_6$) $\delta$: 9.57 (m, 1H, NH), 8.69 (s, 1H, NH), 7.68 (m, 10H, ArH), 3.75 (s, 6H, $CH_2$), 2.72 (m, 2H, $CH_2$), 2.27 (s, 6H, $CH_3 \times 2$); $^{13}C$ NMR (101 MHz, DMSO-$d_6$) $\delta$: 165.45 ($N_2$=C−NH), 164.67 ($N_2$=C−N), 145.54 (ArC), 144.99 (ArC), 137.42 (ArC), 136.49 (ArC), 133.54 (ArC), 133.31 (ArC), 133.01 (ArC), 128.59 (ArC), 127.88 (ArC), 126.88 (ArC), 119.70 (C≡N), 110.26 (ArC), 102.84 (ArC), 45.90 ($NCH_2$), 44.46 ($HNCH_2$), 19.07 ($CH_3$); HRMS Calcd. for $C_{29}H_{27}N_9$ $[M+H]^+$: 502.2462, Found: 502.2453.

*4.1.3.20. 4′-((4-((4-Cyanophenyl)amino)-6-(4-methylpiperazin-1-yl)-1,3,5-triazin-2-yl)amino)-3′,5′-dimethyl-[1,1′-biphenyl]-4-carbonitrile (**6i**).* Yield 74%; white solid; m.p. 224–226 °C (EA/PE); IR: $\upsilon$ 3295, 2221, 1744, 1608, 1472 $cm^{-1}$; $^1H$ NMR (400 MHz, DMSO-$d_6$) $\delta$: 9.59−9.51 (m, 1H, NH), 8.69 (d, $J$ = 9.8 Hz, 1H, NH), 8.09−7.43 (m, 10H, ArH), 4.76 (m, 1H, CH), 4.29 (s, 1H, $CH_2$), 3.78 (s, 2H, $CH_2$), 3.39 (s, 3H, $NCH_3$), 2.39 (s, 1H, $CH_2$), 2.26 (s, 7H, $CH_2$, $CH_3 \times 2$), 1.81 (s, 1H, $CH_2$), 1.38 (s, 1H, $CH_2$); $^{13}C$ NMR (101 MHz, DMSO-$d_6$) $\delta$: 165.83 ($N_2$=C−NH), 164.86 ($N_2$=C−N), 145.49 (ArC), 144.96 (ArC), 137.66 (ArC), 137.58 (ArC), 137.40 (ArC), 136.44 (ArC), 135.92 (ArC), 133.27 (ArC), 132.96 (ArC), 127.83 (ArC), 126.83 (ArC), 119.93 (ArC), 119.42 (C≡N), 110.22 (ArC), 102.80 (ArC), 66.49 ($NCH_2$), 54.85 ($NCH_2$), 46.24 ($CH_3NCH_2$), 43.17 ($CH_3NCH_2$), 34.53 ($CH_3N$), 19.05 ($CH_3$); HRMS Calcd. for $C_{30}H_{29}N_9$ $[M+H]^+$: 516.2619, Found: 516.2610.

*4.1.3.21. 4′-((4-((4-Cyanophenyl)amino)-6-(2-(hydroxymethyl) pyrrolidin-1-yl)-1,3,5-triazin-2-yl)amino)-3′,5′-dimethyl-[1,1′-biphenyl]-4-carbonitrile (**6j**).* Yield 70%; white solid; m.p. 257–259 °C (EA/PE); IR: $\upsilon$ 3318, 2218, 1610, 1567, 1477 $cm^{-1}$; $^1H$ NMR (400 MHz, DMSO-$d_6$) $\delta$: 9.48 (m, 1H, NH), 8.83−8.39 (m, 1H, NH), 8.0−7.38 (m, 10H, ArH), 4.82 (m, 1H, OH), 4.21 (s, 1H, NCH), 3.57 (s, 4H, $CH_2$), 2.26 (s, 6H, $CH_3 \times 2$), 1.94 (m, 4H, $CH_2$); $^{13}C$ NMR (101 MHz, DMSO-$d_6$) $\delta$: 165.54 ($N_2$=C−NH), 164.22 ($N_2$=C−N), 145.67 (ArC), 145.00 (ArC), 137.81 (ArC), 137.57 (ArC), 136.39 (ArC), 133.47 (ArC), 133.27 (ArC), 132.96 (ArC), 128.53 (ArC), 128.28 (ArC), 127.83 (ArC), 126.84 (ArC), 120.00 (ArC), 119.42 (C≡N), 119.08 (C≡N), 110.21 (ArC), 102.67 (ArC), 61.88 (NCH), 59.18 ($NCH_2$), 58.92 ($HOCH_2$), 47.42 ($CH_2$), 27.90 ($CH_2$), 23.10 ($CH_2$), 19.02 ($CH_3$); HRMS Calcd. for $C_{30}H_{28}N_8O$ $[M+Na]^+$: 539.2278, Found: 539.2273.

*4.1.3.22. 4′-((4-((4-Cyanophenyl)amino)-6-(3-hydroxypyrrolidin-1-yl)-1,3,5-triazin-2-yl)-amino)-3′,5′-dimethyl-[1,1′-biphenyl]-4-carbonitrile (**6k**).* Yield 75%; white solid; m.p.>300 °C (EA/PE); IR: $\upsilon$ 3387, 2225, 1608, 1576, 1568 $cm^{-1}$; $^1H$ NMR (400 MHz, DMSO-$d_6$) $\delta$: 9.52 (m, 1H, NH), 8.61 (m, 1H, NH), 8.09−7.48 (m, 10H, ArH), 5.03 (s, 1H, OH), 4.38 (s, 1H, OHCH), 3.58 (s, 4H, $CH_2$), 2.26 (s, 6H, $CH_3 \times 2$), 1.95 (m, 2H, $CH_2$); $^{13}C$ NMR (101 MHz, DMSO-$d_6$) $\delta$: 165.51 ($N_2$=C−NH), 164.33 ($N_2$=C−NH), 164.17 ($N_2$=C−N), 145.73 (ArC), 145.01 (ArC), 137.60 (ArC), 136.37 (ArC), 133.28 (ArC), 132.94 (ArC), 127.84 (ArC), 126.84 (ArC), 120.01 (ArC), 119.39 (C≡N), 110.19 (ArC), 102.62 (ArC), 69.30 ($NCH_2$), 55.01 ($NCH_2$), 44.56 (HOCH), 33.64 ($CH_2$), 19.03 ($CH_2$); HRMS Calcd. for $C_{29}H_{26}N_8O$ $[M+Na]^+$: 525.2122, Found: 525.2116.

*4.1.3.23. 4′-((4-((4-Cyanophenyl)amino)-6-(4-hydroxypiperidin-1-yl)-1,3,5-triazin-2-yl)-amino)-3′,5′-dimethyl-[1,1′-biphenyl]-4-carbonitrile (**6l**).* Yield 68%; white solid; m.p. 229–231 °C (EA/PE); IR: $\upsilon$ 3293, 2230, 2218, 1608, 1474 $cm^{-1}$; $^1H$ NMR

(400 MHz, DMSO-$d_6$) $\delta$: 9.55 (m, 1H, NH), 8.68 (s, 1H, NH), 8.04−7.47 (m, 10H, ArH), 4.74 (m, 1H, OH), 4.28 (s, 2H, $CH_2$), 3.72 (m, 1H, OHCH), 3.34−3.26 (m, 2H, $CH_2$), 2.26 (s, 6H, $CH_3 \times 2$), 1.81 (s, 2H, $CH_2$), 1.30 (m, 2H, $CH_2$); $^{13}$C NMR (101 MHz, DMSO-$d_6$) $\delta$: 165.87 ($N_2$═C−NH), 164.82 ($N_2$═C−N), 145.54 (ArC), 144.98 (ArC), 137.66 (ArC), 137.39 (ArC), 136.65 (ArC), 133.28 (ArC), 132.96 (ArC), 127.84 (ArC), 126.84 (ArC), 119.68 (C≡N), 110.21 (ArC), 102.75 (ArC), 66.47 ($NCH_2$), 34.53 (HOCH), 19.05 ($CH_3$); HRMS Calcd. for $C_{30}H_{28}N_8O$ $[M+Na]^+$: 539.2278, Found: 539.2272.

*4.1.3.24. 4′-((4-((4-Cyanophenyl)amino)-6-((2-morpholinoethyl)amino)-1,3,5-triazin-2-yl)-amino)-3′,5′-dimethyl-[1,1′-biphenyl]-4-carbonitrile (**6m**).* Yield 70%; white solid; m.p. 190–192 °C (EA/PE); IR: $\upsilon$ 3289, 2222, 1607, 1570, 1479 cm$^{-1}$; $^1$H NMR (400 MHz, DMSO-$d_6$) $\delta$: 9.49 (m, 1H, NH), 8.55 (m, 1H, NH), 8.07−7.39 (m, 10H, ArH), 6.94 (m, 1H, NH), 3.53 (m, 5H, $CH_2$), 3.30 (s, 1H, CH), 2.50−2.00 (m, 12H, $CH_2$, $CH_3 \times 2$); $^{13}$C NMR (101 MHz, DMSO-$d_6$) $\delta$: 166.19 ($N_2$═C−NH), 165.41 ($N_2$═C−NH), 164.67 ($N_2$═C−NH), 145.68 (ArC), 144.96 (ArC), 137.57 (ArC), 136.41 (ArC), 133.28 (ArC), 132.90 (ArC), 127.77 (ArC), 126.84 (ArC), 126.47 (ArC), 119.72 (C≡N), 110.21 (ArC), 102.74 (ArC), 66.69 ($HNCH_2$), 58.01 ($NCH_2$), 53.66 ($NCH_2$), 37.73 ($OCH_2$), 37.15 ($OCH_2$), 18.98 ($CH_3$); HRMS Calcd. for $C_{31}H_{31}N_9O$ $[M+H]^+$: 546.2724, Found: 546.2727.

*4.1.3.25. 4′-((4-((4-Cyanophenyl)amino)-6-((2-(4-methylpiperazin-1-yl)ethyl)amino)-1,3,5-triazin-2-yl)amino)-3′,5′-dimethyl-[1,1′-biphenyl]-4-carbonitrile (**6n**).* Yield 69%; white solid; m.p. 180–182 °C (EA/PE); IR: $\upsilon$ 2938, 2222, 1606, 1568, 1477 cm$^{-1}$; $^1$H NMR (400 MHz, DMSO-$d_6$) $\delta$: 9.48 (m, 1H, NH), 8.54 (m, 1H, NH), 8.07−7.47 (m, 10H, ArH), 6.91 (m, 1H, NH), 3.43 (s, 3H, $NCH_3$), 2.51−1.91 (m, 18H, $CH_2$, $CH_3 \times 2$); $^{13}$C NMR (101 MHz, DMSO-$d_6$) $\delta$: 166.18 ($N_2$═C−NH), 164.75 ($N_2$═C−NH), 145.68 ($N_2$═C−NH), 144.96 (ArC), 137.49 (ArC), 136.41 (ArC), 133.09 (ArC), 127.84 (ArC), 126.83 (ArC), 120.03 (ArC), 119.41 (C≡N), 110.21 (ArC), 57.55 ($HNCH_2$), 55.20 ($NCH_2$), 53.17 ($NCH_2$), 52.86 ($NCH_2$), 46.18 ($NCH_3$), 38.06 ($NCH_2$), 37.48 ($NCH_2$), 18.98 ($CH_3$); HRMS Calcd. for $C_{32}H_{34}N_{10}$ $[M+H]^+$: 559.3041, Found: 559.3034.

### *4.2. Other protocols*

Other experimental method including biological testing methods and molecular dynamic methods are described in Supporting Information associated with this article.

## Acknowledgments

This research work was financially supported by National Natural Science Foundation of China under Grant Nos. 21871055 and 21372050 as well as Shanghai Municipal Natural Science Foundation under Grant No. 13ZR1402200 (China). We would like to thank the technical assistance of Mr. Kris Uyttersprot, Mrs. Kristien Erven, and Mrs. Cindy Heens from the Rega Instititute of Leuven University for the HIV experiments and HIV RT polymerase assays.

## Author contributions

Kaijun Jin and Minjie Liu synthesized the compounds. Chunlin Zhuang helped to edit the article. Erik De Clercq and Christophe Pannecouque completed the biological evaluation. Ge Meng was in charge of writing this article and summarizing the data. Fener Chen is the tutor of Kaijun Jin.

## Conflicts of interest

The authors have no conflicts of interest to declare.

## Appendix A. Supporting information

Supporting data to this article can be found online at https://doi.org/10.1016/j.apsb.2019.09.007.

## References

1. de Clercq E. New anti-HIV agents and targets. *Med Res Rev* 2002;**22**:531−65.
2. Zhang X. Anti-retroviral drugs: current state and development in the next decade. *Acta Pharm Sin B* 2018;**8**:131−6.
3. Song Y, Fang Z, Zhan P, Liu X. Recent advances in the discovery and development of novel HIV-1 NNRTI platforms (Part II): 2009−2013 update. *Curr Med Chem* 2013;**21**:329−55.
4. de Béthune M. Non-nucleoside reverse transcriptase inhibitors (NNRTIs), their discovery, development, and use in the treatment of HIV-1 infection: a review of the last 20 years (1989−2009). *Antivir Res* 2010;**85**:75−90.
5. Bec G, Meyer B, Gerard MA, Steger J, Fauster K, Wolff P, et al. Thermodynamics of HIV-1 reverse transcriptase in action elucidates the mechanism of action of non-nucleoside inhibitors. *J Am Chem Soc* 2013;**135**:9743−52.
6. Rawal RK, Murugesan V, Katti SB. Structure−activity relationship studies on clinically relevant HIV-1 NNRTIs. *Curr Med Chem* 2012;**19**:5364−80.
7. Wang J, Morin P, Wang W, Kollman PA. Use of MM-PBSA in reproducing the binding free energies to HIV-1 RT of TIBO derivatives and predicting the binding mode to HIV-1 RT of efavirenz by docking and MM-PBSA. *J Am Chem Soc* 2001;**123**:5221−30.
8. Tantillo C, Ding J, Jacobo-Molina A, Nanni RG, Boyer PL, Hughes SH, et al. Locations of anti-AIDS drug binding sites and resistance mutations in the three-dimensional structure of HIV-1 reverse transcriptase. *J Mol Biol* 1994;**243**:369−87.
9. Dodda LS, Tirado-Rives J, Jorgensen WL. Unbinding dynamics of non-nucleoside inhibitors from HIV-1 reverse transcriptase. *J Phys Chem B* 2019;**123**:1741−8.
10. Ekkati AR, Bollini M, Domaoal RA, Spasov KA, Anderson KS, Jorgensen WL. Discovery of dimeric inhibitors by extension into the entrance channel of HIV-1 reverse transcriptase. *Bioorg Med Chem Lett* 2012;**22**:1565−8.
11. Bollini M, Frey KM, Cisneros JA, Spasov KA, Das K, Bauman JD, et al. Extension into the entrance channel of HIV-1 reverse transcriptase—crystallography and enhanced solubility. *Bioorg Med Chem Lett* 2013;**23**:5209−12.
12. Meng G, Chen F, de Clercq E, Balzarini J, Pannecouque C. Non-nucleoside HIV-1 reverse transcriptase inhibitors: part i. synthesis and structure−activity relationship of 1-alkoxymethyl-5-alkyl-6-naphthylmethyl uracils as HEPT analogues. *Chem Pharm Bull* 2003;**51**:779−89.
13. Das K, Clark Jr AD, Lewi PJ, Heeres J, de Jonge MR, Koymans LM, et al. Roles of conformational and positional adaptability in structure-based design of TMC125-R165335 (etravirine) and related non-nucleoside reverse transcriptase inhibitors that are highly potent and effective against wild-type and drug-resistant HIV-1 variants. *J Med Chem* 2004;**47**:2550−60.
14. Das K, Bauman JD, Rim AS, Dharia C, Clark Jr AD, Camarasa MJ, et al. Crystal structure of *tert*-butyldimethylsilyl-spiroaminooxathioledioxide-thymine (TSAO-T) in complex with HIV-1 reverse

transcriptase (RT) redefines the elastic limits of the non-nucleoside inhibitor-binding pocket. *J Med Chem* 2011;**54**:2727−37.
15. Paris KA, Haq O, Felts AK, Das K, Arnold E, Levy RM. Conformational landscape of the human immunodeficiency virus type 1 reverse transcriptase non-nucleoside inhibitor binding pocket: lessons for inhibitor design from a cluster analysis of many crystal structures. *J Med Chem* 2009;**52**:6413−20.
16. Ariën KK, Venkatraj M, Michiels J, Joossens J, Vereecken K, Van der Veken P, et al. Diaryltriazine non-nucleoside reverse transcriptase inhibitors are potent candidates for pre-exposure prophylaxis in the prevention of sexual HIV transmission. *J Antimicrob Chemother* 2013;**68**:2038−47.
17. Chen X, Zhan P, Li D, de Clercq E, Liu X. Recent advances in dapys and related analogues as HIV-1 NNRTIs. *Curr Med Chem* 2011;**18**:359−76.
18. Zhan P, Chen X, Li D, Fang Z, de Clercq E, Liu X. HIV-1 NNRTIs: structural diversity, pharmacophore similarity, and impliations for drug design. *Med Res Rev* 2013;**33**:E1−72.
19. Janssen PA, Lewi PJ, Arnold E, Daeyaert F, de Jonge M, Heeres J, et al. In search of a novel anti-HIV drug: multidisciplinary coordination in the discovery of 4-[[4-[[4-[(1*E*)-2-cyanoethenyl]-2,6-dimethylphenyl]amino]-2-pyrimidinyl]amino]benzonitrile (R278474, rilpivirine). *J Med Chem* 2005;**48**:1901−9.
20. Ludovici DW, Kavash RW, Kukla MJ, Ho CY, Ye H, de Corte BL, et al. Evolution of anti-HIV drug candidates. Part 2: diaryltriazine (DATA) analogues. *Bioorg Med Chem Lett* 2001;**11**:2229−34.
21. Lansdon EB, Brendza KM, Hung M, Wang R, Mukund S, Jin D, et al. Crystal structures of HIV-1 reverse transcriptase with etravirine (TMC125) and rilpivirine (TMC278): implications for drug design. *J Med Chem* 2010;**53**:4295−9.
22. Wainberg MA, Zaharatos GJ, Brenner BG. Development of antiretroviral drug resistance. *N Engl J Med* 2011;**365**:637−46.
23. Lai MT, Feng M, Falgueyret JP, Tawa P, Witmer M, DiStefano D, et al. *In vitro* characterization of MK-1439, a novel HIV-1 nonnucleoside reverse transcriptase inhibitor. *Antimicrob Agents Chemother* 2014;**58**:1652−63.
24. Xiong Y, Chen F, Balzarini J, de Clercq E, Pannecouque C. Non-nucleoside HIV-1 reverse transcriptase inhibitors. Part 11: structural modulations of diaryltriazines with potent anti-HIV activity. *Eur J Med Chem* 2008;**43**:1230−6.
25. Xiong Y, Chen F, Balzarini J, de Clercq E, Pannecouque C. Non-nucleoside HIV-1 reverse transcriptase inhibitors. Part 13: synthesis of fluorine-containing diaryltriazine derivatives for *in vitro* anti-HIV evaluation against wild-type strain. *Chem Biodivers* 2009;**6**:561−8.
26. Li Z, Han J, Chen H. Revealing interaction mode between HIV-1 reverse transcriptase and diaryltriazine analog inhibitor. *Chem Biol Drug Des* 2008;**72**:350−9.
27. Jin K, Yin H, de Clercq E, Pannecouque C, Meng G, Chen F. Discovery of biphenyl-substituted diarylpyrimidines as non-nucleoside reverse transcriptase inhibitors with high potency against wild-type and mutant HIV-1. *Eur J Med Chem* 2018;**145**:726−34.
28. Sang Y, Han S, Pannecouque C, de Clercq E, Zhuang C, Chen F. Conformational restriction design of thiophene-biphenyl-DAPY HIV-1 non-nucleoside reverse transcriptase inhibitors. *Eur J Med Chem* 2019;**182**:111603.
29. Sang Y, Han S, Han S, Pannecouque C, de Clercq E, Zhuang C, et al. Follow on-based optimization of the biphenyl-DAPYs as HIV-1 non-nucleoside reverse transcriptase inhibitors against the wild-type and mutant strains. *Bioorg Chem* 2019;**89**:102974.
30. Gu S, Xiao T, Zhu Y, Liu G, Chen F. Recent progress in HIV-1 inhibitors targeting the entrance channel of HIV-1 non-nucleoside reverse transcriptase inhibitor binding pocket. *Eur J Med Chem* 2019;**174**:277−91.
31. Du Z, Zhou W, Wang F, Wang J. *In situ* generation of palladium nanoparticles: ligand-free palladium catalyzed ultrafast Suzuki−Miyaura cross-coupling reaction in aqueous phase at room temperature. *Tetrahedron* 2011;**67**:4914−8.
32. Lu D, Chambers P, Wipf P, Xie X, Englert D, Weber S. Lipophilicity screening of novel drug-like compounds and comparison to clog*P*. *J Chromatogr A* 2012;**1258**:161−7.
33. Namasivayam V, Vanangamudi M, Kramer VG, Kurup S, Zhan P, Liu X, et al. The journey of HIV-1 non-nucleoside reverse transcriptase inhibitors (NNRTIs) from lab to clinic. *J Med Chem* 2019;**62**:4851−83.
34. Liu X, Wright M, Hop CE. Rational use of plasma protein and tissue binding data in drug design. *J Med Chem* 2014;**57**:8238−48.
35. Abraham MJ, Murtola T, Schulz R, Páll S, Smith JC, Hess B, et al. GROMACS: high performance molecular simulations through multi-level parallelism from laptops to supercomputers. *Software* 2015;**1-2**:19−25.